



OPEN ACCESS

EDITED BY

Yan Li,
Florida State University, United States

REVIEWED BY

Xiaoping Bao,
Purdue University, United States
Yong Yang,
University of North Texas, United States

*CORRESPONDENCE

Yuguo Lei,
yxl6034@psu.edu

*These authors have contributed equally to this work

SPECIALTY SECTION

This article was submitted to
Biochemical Engineering,
a section of the journal
Frontiers in Chemical Engineering

RECEIVED 30 August 2022

ACCEPTED 04 October 2022

PUBLISHED 20 October 2022

CITATION

Li Q, Pan Y, Han L, Yang Y, Wu X and Lei Y (2022), Improving three-dimensional human pluripotent cell culture efficiency via surface molecule coating. *Front. Chem. Eng.* 4:1031395. doi: 10.3389/fceng.2022.1031395

COPYRIGHT

© 2022 Li, Pan, Han, Yang, Wu and Lei. This is an open-access article distributed under the terms of the [Creative Commons Attribution License \(CC BY\)](https://creativecommons.org/licenses/by/4.0/). The use, distribution or reproduction in other forums is permitted, provided the original author(s) and the copyright owner(s) are credited and that the original publication in this journal is cited, in accordance with accepted academic practice. No use, distribution or reproduction is permitted which does not comply with these terms.

Improving three-dimensional human pluripotent cell culture efficiency *via* surface molecule coating

Qiang Li^{1†}, Ying Pan^{2†}, Li Han^{2†}, Yakun Yang², Xinran Wu² and Yuguo Lei^{1,2,3*}

¹Department of Chemical and Biomolecular Engineering, University of Nebraska, Lincoln, NE, United States, ²Department of Biomedical Engineering, Pennsylvania State University, University Park, PA, United States, ³Huck Institutes of the Life Sciences, Pennsylvania State University, University Park, PA, United States

Human pluripotent stem cells (hPSCs) are ideal “raw materials” for making various human cell types for regenerative medicine and are needed in large numbers. 3D suspension culturing (e.g., stirred-tank bioreactor or STR), which suspends and cultures cells in an agitated medium, has been extensively studied to scale up hPSC production. However, a significant problem with 3D suspension is the uncontrolled spheroid agglomeration. It leads to cell growth arrest, cell apoptosis, and inhomogeneity in cell purity and quality. We propose that i) inhibiting the spheroid adhesion can prevent spheroid agglomeration and ii) the inhibition can be achieved *via* coating spheroids with biocompatible anti-adhesion molecules. We used PEG-lipids as model anti-adhesion molecules to successfully demonstrate the concept. PEG-lipids anchor to the spheroid surface through the interactions between their lipid chains and the cell membrane lipids. The flexible and hydrophilic PEG chains act as a dynamic barrier to prevent spheroid adhesion. We showed that the coating eliminated spheroid agglomeration, leading to homogenous spheroid size distribution and significant improvements in cell growth rate and volumetric yield. This novel approach is expected to impact large-scale hPSC production significantly. Furthermore, the approach can be generalized for culturing other human cell types.

KEYWORDS

human pluripotent stem cells, three-dimensional culture, surface coating, surfactant, poly (ethylene glycol)

Introduction

Eighty percent of healthcare costs are used to treat late-stage illnesses, which could be treated or managed early through regenerative medicine (Denning et al., 2016). Human pluripotent stem cells (hPSCs) including human embryonic stem cells (hESCs) (Thomson et al., 1998) and induced pluripotent stem cells (iPSCs), have unlimited proliferation capability. They can be expanded to generate large numbers of cells. hPSCs also have the

potential to differentiate into all somatic cells (Tabar and Studer, 2014; Kimbrel and Lanza, 2015; Trounson and McDonald, 2015). Thus they are ideal “raw materials” for making various human cell types for regenerative medicine. Since their first report in 1998, hPSCs have been successfully differentiated into various cell types such as cardiomyocytes, beta cells, endothelial cells, vascular smooth muscle cells, muscle cells, neural stem cells, neurons, macrophages, T cells, natural killer cells, etc. (Yamanaka, 2020). hPSC-derived cells have been widely used to model genetic and environmental diseases (Brennan et al., 2011; Devine et al., 2011; Israel et al., 2012; Ambasadhan et al., 2013; Kondo et al., 2013; Reinhardt et al., 2013; Woodruff et al., 2013; Young et al., 2015; Soldner et al., 2016). They have been applied for screening new drugs (Höing et al., 2012; Naryshkin et al., 2014; Bright et al., 2015; Kumari et al., 2015; McNeish et al., 2015), testing drug toxicity (Matsa et al., 2016a; Matsa et al., 2016b; Burrige et al., 2016; Kodo et al., 2016; Sayed et al., 2016; Sharma et al., 2017; Magdy et al., 2018), engineering tissues, and developing cell-based therapies (Barker et al., 2017; Kikuchi et al., 2017; Mandai et al., 2017). Several clinical trials using hPSC derivatives are ongoing (Mandai et al., 2017; Deinsberger et al., 2020).

However, the widespread use of hPSCs and their derivatives is limited by the difficulty of producing them on large scales at high quality (Jenkins and Farid, 2015; Mount et al., 2015; Silva et al., 2015; Denning et al., 2016; Hartman et al., 2016; Kempf et al., 2016; National science and technology council, 2016). Regenerative medicine needs large numbers of cells (Lei and Schaffer, 2013; Denning et al., 2016; Kempf et al., 2016). For instance, $\sim 1 \times 10^{10}$ cardiomyocytes or beta cells for treating a myocardial infarction or diabetic patient (Amour et al., 2006; Serra et al., 2012; Chong et al., 2014), 1×10^{11} platelets for a platelet transfusion (Amour et al., 2006; Serra et al., 2012; Chong et al., 2014), $\sim 1 \times 10^{10}$ cardiomyocytes for making a human heart (Badylak et al., 2011), and $\sim 1 \times 10^{10}$ cells for screening one million compounds (Desbordes and Studer, 2012). Regenerative medicine also requires cells to have high quality, such as normal genetics, epigenetics, phenotypes, and high *in vivo* safety and functions (Lei and Schaffer, 2013; Denning et al., 2016; Kempf et al., 2016). hPSC-derived cells can be prepared as universal cells and used as off-shelf products (i.e., allogeneic cells). This approach requires the capability to culture massive numbers of cells per batch (Denning et al., 2016; Hartman et al., 2016; Kempf et al., 2016). Alternatively, patient-specific cells can be prepared for personalized regenerative medicine (i.e., autologous cells). This approach requires a technology to produce cells for thousands of patients in parallel (Trainor et al., 2014). To date, the production of high-quality allogeneic or autologous cells at large scales has not been achieved due to the low efficiency of current cell culture methods (Baum et al., 2013; National Cell Manufacturing Consortium, 2016; National science and technology council, 2016).

hPSCs are typically cultured on a 2D surface. However, 2D culturing is labor- and space-consuming and is only suitable for preparing small numbers of cells (Kropp et al., 2017). Due to its success in culturing Chinese Hamster Ovary (CHO) cells for producing protein therapeutics, 3D suspension culturing (e.g., stirred-tank bioreactor or STR), which suspends and cultures cells in an agitated medium, has been extensively studied to scale up hPSC production (Polak and Mantalaris, 2008; Serra et al., 2012). However, a significant problem with 3D suspension is the uncontrolled cellular aggregation. hPSCs have strong cell-cell interactions (Chen et al., 2014a; Chen et al., 2014b) that make them aggregate to form large cell agglomerates in suspension (Kinney et al., 2011; Fridley et al., 2012; Kropp et al., 2017). The mass transport in agglomerates $>500 \mu\text{m}$ in diameter becomes insufficient, leading to cell growth arrest, apoptosis, and uncontrolled differentiation (Hajdu et al., 2010; Kropp et al., 2017). Additionally, uncontrolled cellular aggregation leads to inhomogeneity in hPSC aggregate or spheroid size. Since the spheroid size significantly influences the hPSC differentiation efficiency (Jara-avaca et al., 2014; Kropp et al., 2017), the inhomogeneity in aggregate size results in heterogeneity in product purity (Jara-avaca et al., 2014; Kropp et al., 2017).

In short, uncontrolled cellular aggregation should be mitigated to improve the hPSC culture efficiency and product homogeneity in 3D suspension culture. This report proposes to coat hPSC spheroids with biocompatible anti-adhesion molecules to reduce spheroid agglomeration. To our best knowledge, this is the first report to propose and successfully demonstrate using a molecular coating to reduce spheroid agglomeration to enhance hPSC culture efficiency. We believe this novel approach will have a significant impact on large-scale hPSC production.

Materials and methods

Materials

E8 medium (E8), accutase and Live/Dead cell viability staining kit: Life Technologies; Y-27632: Selleckchem; Matrigel: BD Biosciences; Calcein AM viability dye (#50-169-52, eBioscience); Ethidium homodimer I (#40010, Biotium); Antibodies for Nanog, Oct4, SSEA-4 and Alkaline phosphatase (R&D system, 10 $\mu\text{g}/\text{ml}$); Nestin antibody (BioLegend, 1:200); α -SMA antibody (Santa Cruz, 1:200); FOXA2 antibody (Santa Cruz, 1:200); Polyethylene Glycol conjugated with 1,2-Dipalmitoyl-sn-Glycero-3-Phosphoethanolamine (PEG-DPPE, Mw5000, #PG1-DP-5k, Nanocs); Polyethylene Glycol conjugated with 1,2-Distearoyl-sn-Glycero-3-Phosphoethanolamine (PEG-DSPE, Mw5000, #PG1-DS-5k, Nanocs); Fluorescein labeled DSPE-PEG (DSPE-PEG-FITC, Mw 5,000, PG2-DSFC-5k, Nanocs); Fluorescein

Phenylindole, Dihydrochloride (DAPI) were added and incubated for another 1 h at room temperature. Finally, cells were washed with PBS 3 times before imaging with a Zeiss Axio Observer Fluorescent Microscopy. LIVE/DEAD[®] Cell Viability staining was used to assess live and dead cells, according to the product manual.

EB differentiation

hPSC spheroids were cultured for five passages with PEG-DPPE and then suspended in DMEM +20% FBS +10 μ M β -mercaptoethanol in a low adhesion plate for 6 days. The cell mass was then transferred onto plates coated with 0.1% gelatin and cultured in the same medium for another 6 days, followed by fixation and staining as above.

Statistical analysis

The data are presented as the mean \pm SD. We used an unpaired *t*-test to compare two groups and one-way ANOVA to compare more than two groups. $p < 0.05$ was considered statistically significant.

Results

Using molecular coating to avoid spheroid agglomeration

3D suspension cultures are being widely studied for culturing hPSCs due to their simplicity, easiness for scaling up, and automation (New Brunswick Scientific et al., 2009; Serra et al., 2012). Ideally, inoculated single hPSCs expand through two phases: single cells first associate to form small cell clusters (i.e., initial clustering) that subsequently expand as spheroids (i.e., cell or spheroid expansion) (Figure 1A). Unfortunately, neighboring spheroids frequently adhere to each other and fuse to form large agglomerates ($>500 \mu\text{m}$, i.e., spheroid agglomeration) (Figure 1A). The initial clustering, spheroid expansion, and spheroid agglomeration were clearly demonstrated in a simple experiment. Two vials of hPSCs, stained with DIO and DID dyes, respectively, were mixed at 1:1 and cultured in suspension. The lipophilic DIO and DID dyes stain cells to appear green and red, respectively, under fluorescent microscopy. Single cells associated to form small clusters in 24 h that subsequently expanded as spheroids. Spheroid agglomeration was frequently found on day 4 (Figure 1B).

It is well known that the transport of nutrients, oxygen, and growth factors to cells located at the center of agglomerates with diameters larger than $500 \mu\text{m}$ becomes insufficient (Hajdu et al., 2010; Kropp et al., 2017). Therefore, the large cell spheroids

exhibit a layer-like structure, including a necrotic core and an outer layer of live cells (Alvarez-Pérez et al., 2005; Lin and Chang, 2008). This was confirmed in our experiment. We prepared hPSC spheroids with diameters of $200 \mu\text{m}$, $400 \mu\text{m}$, $500 \mu\text{m}$, $700 \mu\text{m}$, and $800 \mu\text{m}$ and cultured them for 3 days (Figure 2). Live/dead staining showed very few dead cells in spheroids $<400 \mu\text{m}$ and significant dead cells in spheroids $\geq 500 \mu\text{m}$. Large necrotic cores appeared when the spheroid's diameter exceeded $700 \mu\text{m}$ (Figures 2C, D). Therefore, uncontrolled cell aggregation ($>500 \mu\text{m}$) is a critical problem for 3D suspension culture (Lei and Schaffer, 2013; Lei et al., 2014; Li et al., 2018). The above mechanistic studies clearly show that if hPSCs could follow the initial clustering-spheroid expansion path without spheroid agglomeration, the resultant spheroids would have uniform size, and the cell growth rate, viability, yield, and quality could be maximized.

To find a solution to prevent spheroid agglomeration, we must understand the molecular mechanisms under cell aggregation and spheroid agglomeration. On the plasma membranes of single cells or cells on the spheroid surface, many cell-cell adhesion molecules (e.g., cadherins) and receptors for ECM proteins (e.g., integrins) are not bound by their ligands (Foty and Steinberg, 2005). These molecules drive cells to aggregate to maximize their interactions with their ligands (Ivascu and Kubbies, 2006; Pérez-Pomares and Foty, 2006; Ivascu and Kubbies, 2007). Cells can aggregate through, individually or combined, cell-cell adhesions and cell-matrix interactions. Through these mechanisms, single hPSCs associate to form small clusters. During the cell expansion in suspension cultures, and when two spheroids contact, cells on one spheroid can adhere to cells or ECMs of the other spheroid through cell-cell, cell-matrix interactions, leading to spheroid adhesion and agglomeration.

We propose that i) inhibiting the spheroid adhesion can prevent spheroid agglomeration and ii) the inhibition can be achieved *via* coating the spheroids with a layer of biocompatible anti-adhesion molecules (Figure 1C). This study will use Polyethylene glycol conjugated with lipids (PEG-lipids) as model anti-adhesion molecules to demonstrate the concept. The PEG-lipids can anchor to the spheroid surface through the interactions between their lipid chains and the cell membrane lipids (Tatsumi et al., 2012). The flexible and hydrophilic PEG chains act as a dynamic barrier to prevent spheroid adhesion.

Spheroid fusion assay

We developed a spheroid fusion assay for quantitatively studying spheroid agglomeration. To generate hPSC spheroids, single cells were suspended in V-bottom low attachment 96-well plates. Within hours, single cells settled at the well bottom and formed a cell cluster. For the fusion assay,

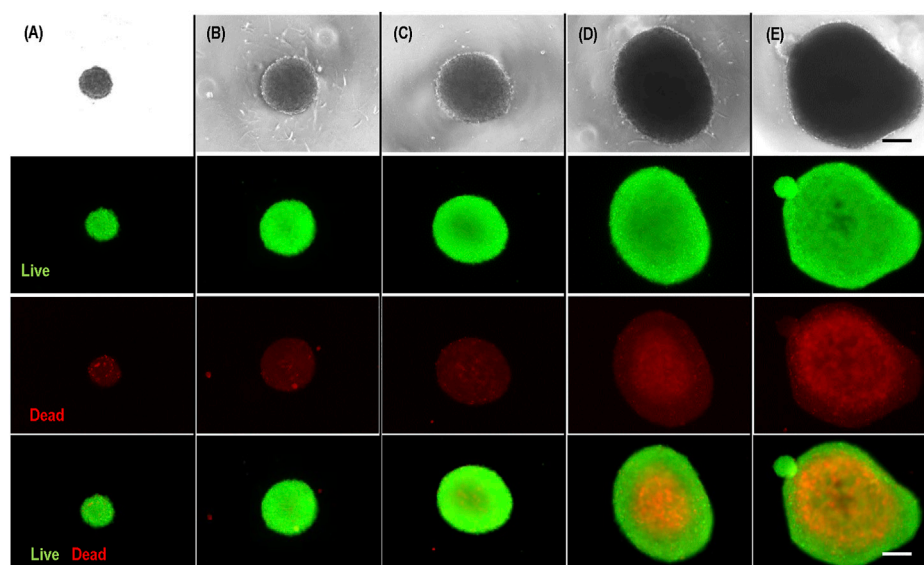


FIGURE 2
Live/dead staining of hPSC spheroids with diameter of 200 μm (A), 400 μm (B), 500 μm (C), 700 μm (D), 800 μm (E). Scale bar: 200 μm .

two spheroids were placed into one low attachment V-shape well (Figure 3A). The fusion process was imaged at 0, 2, 8, and 28 h. We used the $(\pi r^2)/(\pi R^2)$, wherein r and R are the radius of the interface of the two spheroids and the radius of the spheroids, respectively, to quantitatively measure the percentage of the spheroid fusion (Figure 3C). And $t_{1/2}$ is referred to the time when 50% of the fusion is completed or $(\pi r^2)/(\pi R^2) = 0.5$ (Figure 3D). We found that $t_{1/2}$ is less than 5 h. We measured the fusion rates of spheroids with different diameters and found that the spheroid size did not significantly affect the fusion rate (Figures 3B–D).

PEG-lipids coating on hPSC spheroids

PEG-lipids molecules have been reported for surface modification of cells to modulate immunogenicity (Teramura and Iwata, 2010a; Teramura and Iwata, 2010b; Inui et al., 2010; Takemoto et al., 2011; Tatsumi et al., 2012). We first studied if PEG-lipids could coat hPSC spheroids. Spheroids were prepared and treated with PEG-DPPE at varied concentrations for 30 min. Without PEG-DPPE coating, the spheroid surface was smooth, and the cell-to-cell boundaries were not clearly seen (Figures 4A, B). The spheroid surface became rough, and cell-to-cell boundaries became apparent after PEG-DPPE coating. The morphology change indicates that PEG-DPPE coating decreased the spheroid surface tension. The coating did not cause cell death. When treated with 100 $\mu\text{g}/$

ml, 250 $\mu\text{g}/\text{ml}$, 500 $\mu\text{g}/\text{ml}$, very few dead cells were detected (Figure 4C).

To confirm the coating and investigate its stability, we coated spheroids with FITC labeled PEG-DPPE for 30 min and imaged them with a confocal microscope immediately and 24 h after the coating. Fluorescence was clearly observed at the spheroid surface, showing successful coating. However, 24 h later, the fluorescence intensity decreased to about 50%, indicating the half-life time of PEG-DPPE on the spheroid surface was about 24 h (Figure 4D). We treated the spheroids with both 250 $\mu\text{g}/\text{ml}$ and 500 $\mu\text{g}/\text{ml}$ PEG-DPPE and found the coating efficiency and half-life time were similar, indicating 250 $\mu\text{g}/\text{ml}$ was sufficient for coating (Figure 4D). To assess if the lipid length affects the coating stability, we also coated spheroids with FITC labeled PEG-DSPE. The fatty acid DPPE and DSPE have 16 and 18 carbons, respectively. No significant difference was observed between FITC-PEG-DPPE and FITC-PEG-DSPE in terms of the fluorescent intensity immediately and 24 h after coating (Figure 4E).

PEG-lipids coating reduced spheroid agglomeration

We evaluated the effect of PEG-DPPE coating on the spheroid fusion process (Figure 5). Spheroids were generated and treated with 0, 100, 250, and 500 $\mu\text{g}/\text{ml}$ PEG-DPPE for

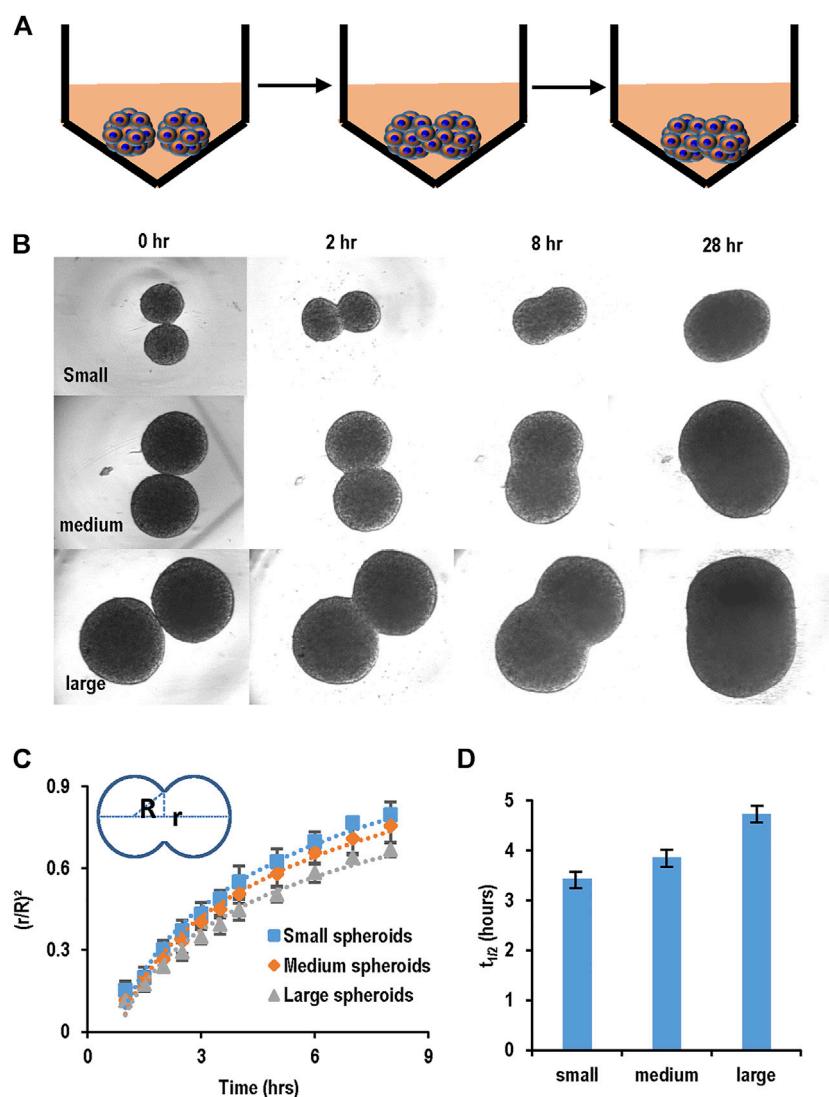


FIGURE 3

Spheroid fusion assay. (A,B) hPSC spheroids with different sizes (small, medium and large) were prepared in V-bottom low attachment 96-well plates, and then two spheroids were placed in contact and the fusion process was imaged using microscopy at 1, 2, 4, 8, and 28 h. (C) The spheroid fusion rates were quantified using $(r/R)^2$, where r and R were the radius of the interface of the two spheroids and the radius of the spheroids, respectively. (D) $t_{1/2}$, the time to complete 50% fusion or $(r/R)^2 = 1/2$. Small, medium and large spheroids had similar fusion rates.

30 min. Two spheroids were placed in one V-shape, and the fusion process was recorded (Figures 5A, B). We found that the fusion rate decreased as the PEG-DPPE concentration increased (Figure 5C). The fusion became extremely slow when treated with 250 or 500 $\mu\text{g/ml}$ PEG-DPPE. The $t_{1/2}$ for spheroids coated with 0, 100, 250, and 500 $\mu\text{g/ml}$ PEG-DPPE was 3.7, 9.2, 26.8, and 69 h, respectively (Figure 5D). We observed that spheroids without coating adhered around 5 min after contacting, and PEG-DPPE coating extended this time to ~ 20 min. Similar results were obtained when PEG-DSPE was used. Thus molecular coating could effectively prevent spheroid adhesion and agglomeration.

PEG-lipids coating prevented spheroid agglomeration in 3D suspension culture

Next, we investigated the effect of PEG-lipids coating in 3D suspension culture. Single cells were suspended in the medium in a low attachment-well plate with shaking at 57 rpm for 24 h to form small cell clusters. The clusters were treated with PEG-DPPE daily, and cultures without PEG-DPPE coating were used as the control. Two initial seeding densities (5×10^5 cells/ml and 1×10^6 cells/ml) were tested to evaluate the effect of seeding density. Two hPSC lines, induced pluripotent stem cells generated from human mesenchymal stem cell cells (MSC-

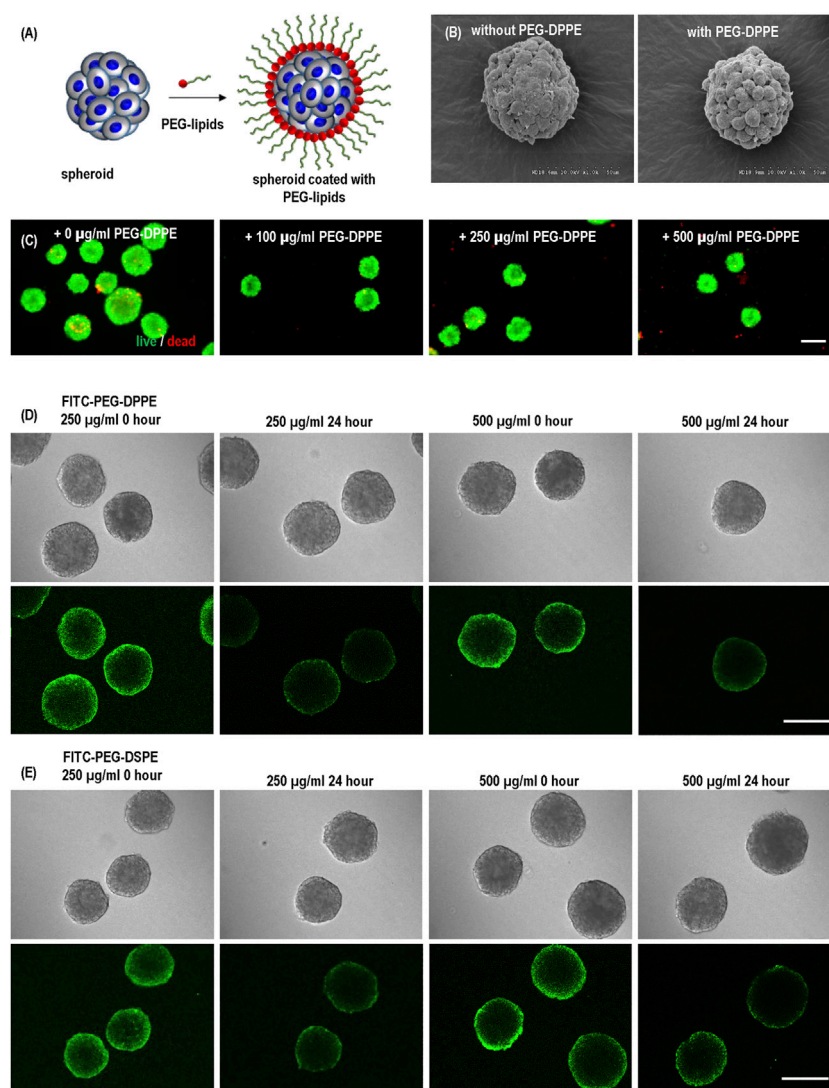


FIGURE 4

(A) hPSC spheroids were coated with PEG-lipids. (B) Scanning electron microscopy images of uncoated and coated spheroids. (C) Live dead staining of spheroids coated with 0, 100, 250, and 500 $\mu\text{g/ml}$ PEG-DPPE. (D,E) Confocal scanning microscopic images of hPSC spheroids coated with 250 and 500 $\mu\text{g/ml}$ FITC-PEG-DPPE (D) or FITC-PEG-DSPE (E). Free PEG-lipids were removed from the medium after coating. Images were taken immediately (0 h) and 24 h after coating. Scale bar: 200 μm .

iPSC) and skin fibroblasts (Fib-iPSC), were studied to assess if the coating method could be cell-line dependent. Cells were harvested daily to analyze the spheroid size, cell number, and cell viability.

For MSC-iPSCs, severe spheroid agglomerations were seen on day 3 and day 4, especially for the high seeding density (Figures 6A, B; Table 1). With the PEG-DPPE coating, uniform cell spheroids were formed at both seeding densities from day 1 to day 4 (Figures 6A, B). We also quantified the size distribution (Figures 6C, D). At low seeding density and without PEG-DPPE coating, the size distribution was 50–121 μm , 65–180 μm , and 85–379 μm , and the median was 90, 121, and 183 μm on day 1, 2,

and 3, respectively. With PEG-DPPE coating, the size distribution became much narrower, e.g., 39–103 μm , 51–124 μm , and 74–178 μm on day 1, 2, and 3, respectively (Figures 6C, D). Moreover, the median became significantly smaller, for instance, 71, 84, and 117 μm on day 1, 2, and 3, respectively (Figures 6C, D). The reductions in mean spheroid size and size distribution by PEG-DPPE coating were also seen at the high seeding density. Without coating, the median was 93, 149, and 189 μm , and the distribution was 51–173 μm , 73–377 μm , and 92–510 μm on day 1, 2, and 3, respectively. With PEG-DPPE coating, the median was 72, 98, and 126 μm , and the size distribution was 41–108 μm , 59–148 μm , and

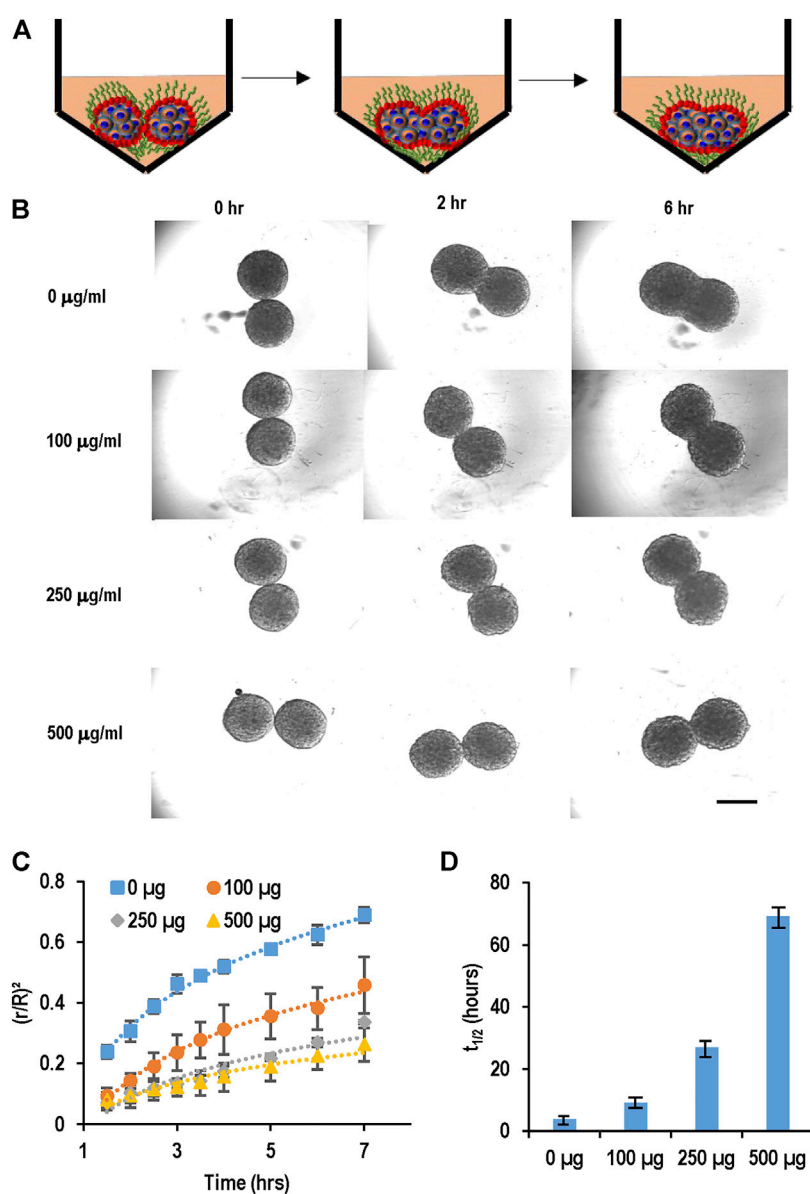


FIGURE 5

PEG-lipids coating slowed down spheroid fusion. (A,B) hPSC spheroids were coated with 0, 100, 250, 500 $\mu\text{g/ml}$ PEG-DPPE, and two spheroids were placed in one well. Their fusion process was recorded with microscopy. (C) The fusion rates and (D) $t_{1/2}$. Scale bar: 200 μm .

76–181 μm on day 1, 2, and 3, respectively. (Figures 6C, D). Large agglomerates were not seen with PEG-DPPE coating.

For both seeding densities without PEG-DPPE coating, the cell number exhibited a slow increase in the first 3 days, and no apparent increase was seen on day 4, resulting in about 2.9- and 1.7-fold expansion after 4 days with a final cell density at 1.5×10^6 cells/ml and 1.7×10^6 cells/ml for 5×10^5 cells/ml and 1×10^6 cells/ml seeding density, respectively, (Figures 6E, F). With PEG-DPPE coating, cells grew in all 4 days, resulting in about 4.9- and 3.3-fold expansion with a final cell density at 2.5×10^6 cells/ml

and 3.3×10^6 cells/ml for 5×10^5 cells/ml and 1×10^6 cells/ml, respectively (Figures 6E, F). Thus the cell expansion and yield were significantly improved by PEG-DPPE coating.

Similar results were achieved when Fib-iPSCs were used (Figure 7, Table 1). PEG-DPPE coating eliminated spheroid agglomeration. When seeded at 5×10^5 cells/ml and without coating, the median was 68, 118, and 183 μm , and the size distribution was 42–136 μm , 53–176 μm , and 76–356 μm on day 1, 2, and 3, respectively, with PEG-DPPE coating, the median was 61, 97, and 139 μm , and the size distributions

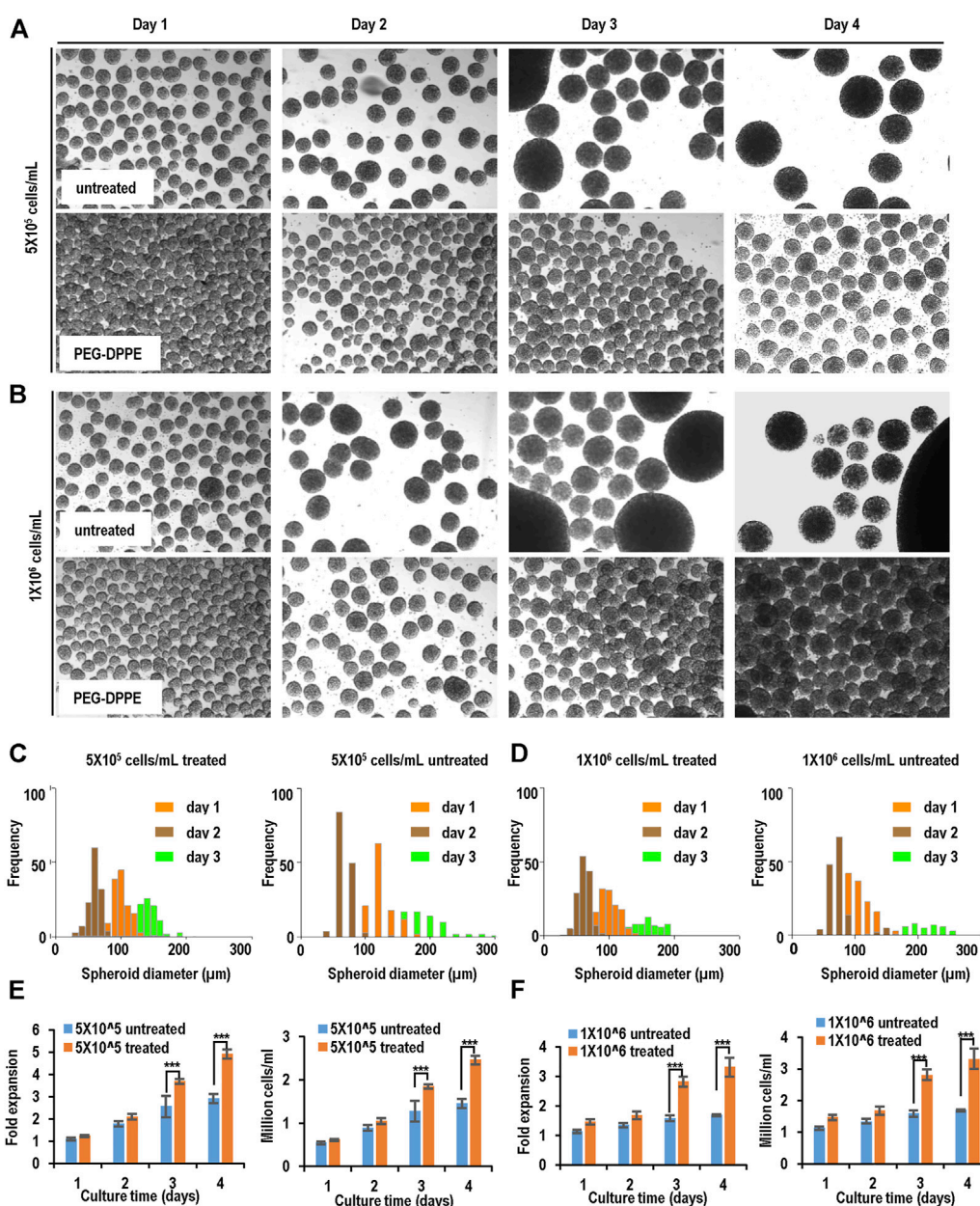


FIGURE 6

Suspension culture of MSC-iPSCs. (A, B) Phase images of spheroids on days 1–4 without and with PEG-DPPE coating at two seeding densities. (C, D) Size distribution of spheroids on days 1–3. (E, F) Fold of expansion and volumetric yield of uncoated and coated cells. ***: $p < 0.001$.

were 27–85 μm , 48–146 μm , and 71–192 μm on day 1, 2, and 3, respectively. When seeded at 1×10^6 cells/ml without PEG-DPPE coating, the median was 71, 133, and 205 μm , and the size distribution was 51–158 μm , 67–322 μm , and 102–456 μm on day 1, 2, and 3, respectively. With PEG-DPPE coating, the median was 62, 98, and 140 μm , and the size distribution was 32–89 μm , 60–169 μm , and 80–195 μm on day 1, 2, and 3, respectively (Figures 7C, D). Without coating, about 3.2- and 1.7-fold expansion with a final cell density at 1.6×10^6 cells/ml

and 1.7×10^6 cells/ml were obtained for 5×10^5 cells/ml and 1×10^6 cells/ml seeding density, respectively. With PEG-DPPE coating, about 5.5- and 3.4-fold expansion with a final cell density at 2.8×10^6 cells/ml and 3.4×10^6 cells/ml were achieved for 5×10^5 cells/ml and 1×10^6 cells/ml seeding density, respectively (Figures 7E, F). In summary, PEG-DPPE coating leads to uniform spheroid formation in 3D suspension culture with significantly improved expansion fold and cell yield.

TABLE 1 Summary of 3D suspension culture results.

Cell Type	Seeding density(Cells/ml)	Coating	Mean diameter(um)			Diameter range(um)			Fold of expansion	Yield (cells/ml)
			day 1	day 2	day 3	day 1	day 2	day 3	day 4	day 4
MSC-iPSCs	5×10 ⁵	no	90	121	183	50-121	65-180	85-379	2.9	1.5×10 ⁶
		PEG-DPPE	71	84	117	39-103	51-124	71-178	4.9	2.5×10 ⁶
	1×10 ⁶	no	93	149	189	51-173	73-377	92-510	1.7	1.7×10 ⁶
		PEG-DPPE	72	98	126	41-108	59-148	76-181	3.3	3.3×10 ⁶
Fib-iPSCs	5×10 ⁵	no	68	118	183	42-136	53-176	76-356	3.2	1.6×10 ⁶
		PEG-DPPE	61	97	139	27-85	48-146	71-162	5.5	2.8×10 ⁶
	1×10 ⁶	no	71	133	205	61-158	67-322	102-456	1.7	1.7×10 ⁶
		PEG-DPPE	32	98	140	32-89	60-169	80-195	3.4	3.6×10 ⁶

hPSCs retained pluripotency after long-term culture with PEG-lipids coating

We cultured hPSCs in suspension with PEG-DPPE coating for 10 passages and evaluated their pluripotency. The PEG-DPPE coating did not sacrifice the pluripotency. Confocal microscope image and flow cytometry analyses showed a majority of cells expressed pluripotency markers after 5 and 10 passages (Figures 8A–C). In addition, *in vitro* embryoid body (EB) differentiation was performed. hPSCs could be differentiated into the Nestin + ectodermal cells, α -SMA + mesodermal cells, and FOXA2+ endodermal cells in the EB assay (Figure 8D). All these results indicate that the PEG-lipids coating support hPSC culture without altering the pluripotency.

Discussion

hPSCs are an ideal cell source for producing various human cell types for regenerative medicine, cell therapy, drug discovery, and disease modeling (Yamanaka, 2020). Large numbers of cells are needed for these applications. 3D suspension is a promising approach to scale up the production (Lei and Schaffer, 2013; Lei et al., 2014; Lin et al., 2017a; Lin et al., 2018a; Lin et al., 2018b; Ekerdt et al., 2018; Li et al., 2018; Lin et al., 2019a; Lin et al., 2019b; Lin et al., 2019d; Wang and Lei, 2019; Wang et al., 2021). However, uncontrolled spheroid agglomeration is a significant problem that negatively affects cell viability, growth rate, yield, and quality in suspension culture. Thus methods to mitigate spheroid agglomeration are valuable and should be developed.

Researchers have tried to optimize the bioprocess parameters, such as the stirring speed, to reduce agglomeration (Kempf et al., 2016). In general, a higher stirring speed reduces spheroids' settlement and agglomeration. However, a high stirring speed results in shear stress, negatively influencing cell viability. In short, this approach can mitigate spheroid agglomeration to a certain level but cannot wholly abolish it (Kempf et al., 2016). We and others have cultured hPSCs in hydrogels with the intention of using hydrogels as physical barriers to eliminate cell agglomeration (Gerecht et al., 2007; Chayosumrit et al., 2010; Serra et al., 2011; Stenberg et al., 2011), but hPSCs have slow growth in most hydrogels. Significantly, we found that a very soft thermoreversible hydrogel enabled the long-term, serial expansion of hPSCs with excellent cell viability, growth rate (20-fold/5 days), and yield ($\sim 2.0 \times 10^7$ cells/ml) (Lei and Schaffer, 2013; Lei et al., 2014; Li et al., 2016; Lin et al., 2017a; Lin et al., 2017b). However, this hydrogel is unstable for long-term and large-scale cell culture. Additionally, the material is expensive and variable between batches.

Our lab also explored using hydrogel tube microbioreactors to prevent agglomeration (Lei and Schaffer, 2013; Lei et al., 2014; Li et al., 2016; Lin et al., 2017a; Lin et al., 2017b). In this method, cells are cultured in microscale hollow hydrogel tubes suspended in a bioreactor. The hydrogel tubes can confine the radial diameter of cell masses within the diffusion limit to ensure efficient mass transport. We showed that hPSCs could grow in hydrogel tubes with high viability (>95%), growth rate (1,000-fold expansion/9 days), pluripotency, and yield (5.0×10^8 cells/ml). However, the hydrogel tubes are incompatible with the existing stirred tank bioreactors since the stirring can break the

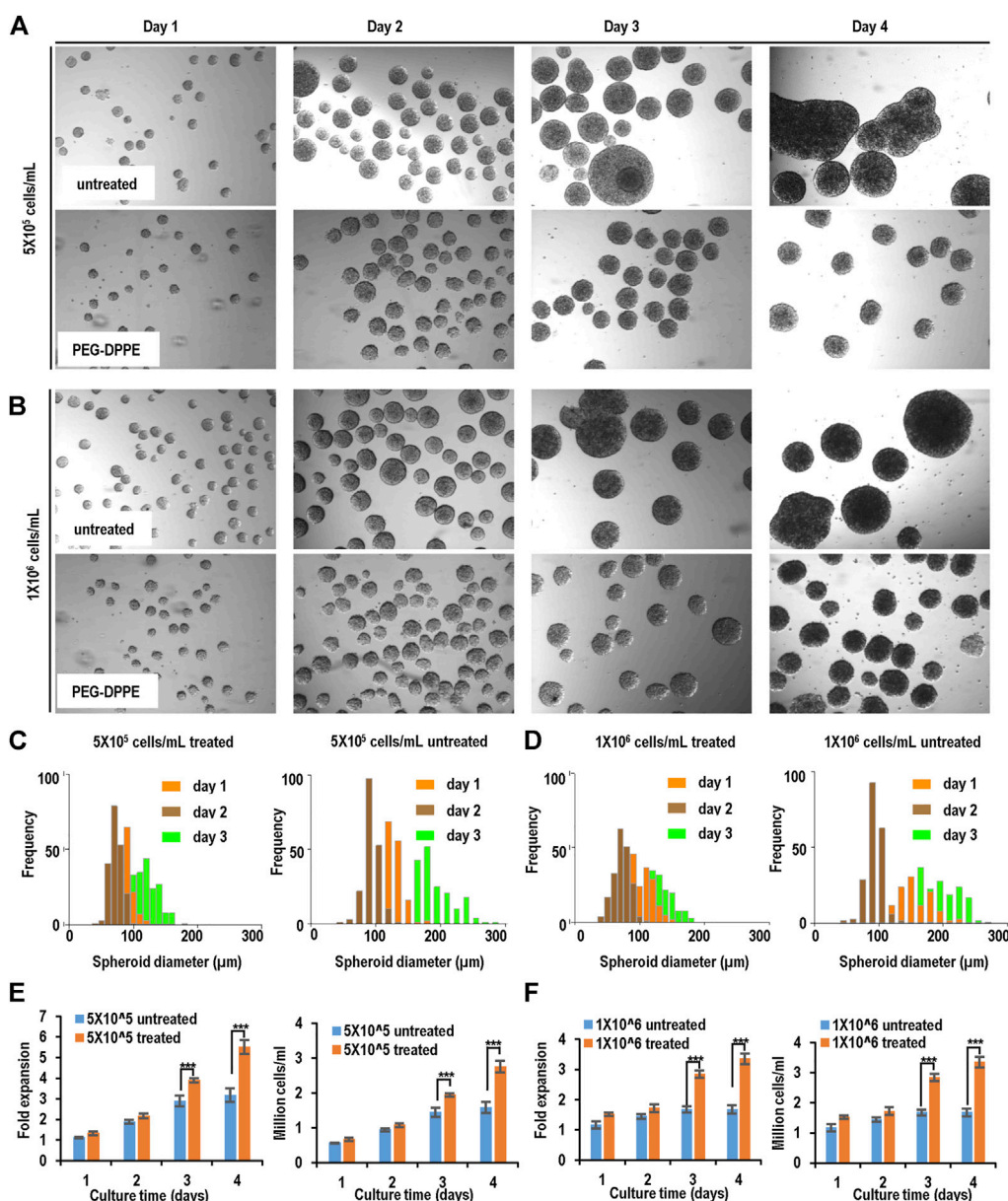


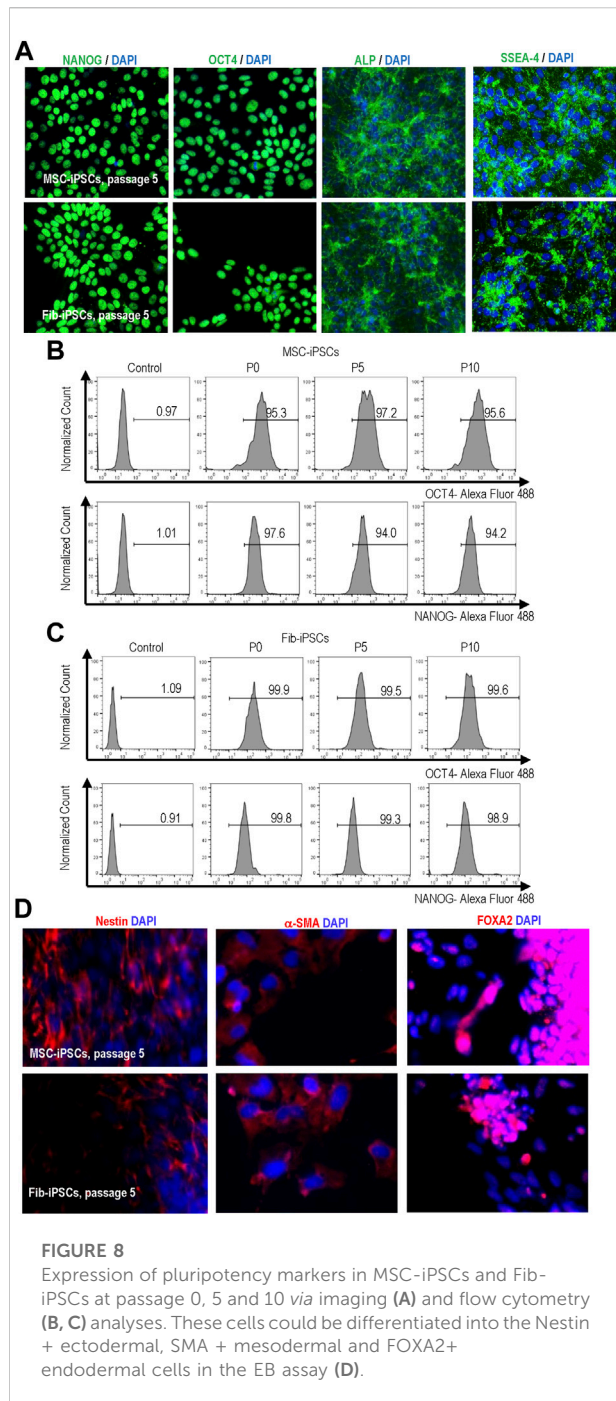
FIGURE 7

Suspension culture of Fib-iPSCs. (A,B) Phase images of spheroids on days 1–4 without and with PEG-DPPE coating at two seeding densities. (C,D) Size distribution of spheroids on days 1–3. (E,F) Fold of expansion and volumetric yield of uncoated and coated cells. ***: $p < 0.001$.

soft hydrogel tubes. Thus special bioreactors should be developed to contain these hydrogel tubes.

In this study, we proposed to use molecular coating to prevent spheroid agglomeration. Compared to the hydrogel tubes, molecular coating is simple and compatible with existing bioreactors. The biocompatible anti-adhesion molecules can be added to the cell culture media as additives. The concept was successfully demonstrated using PEG-lipids.

Spheroid agglomeration was eliminated, resulting in spheroids with uniform size. Consequently, the cell growth rate and volumetric yield were significantly improved. In the future, we can design molecules with better stability and anti-adhesion capabilities to further improve the bioprocess outcome. Although we used lipids to anchor the anti-adhesion molecules in this study, other methods, such as covalent conjugation, ionic binding, and the ligand or antibody-based



affinity binding, can also be used to coat the anti-adhesion molecules. In this study, we used PEG as anti-adhesion molecules. In principle, any biocompatible molecules with anti-adhesion functions can be used. In this study, we focused on culturing hPSCs. In principle, the molecular coating method can be applied to any cell type in suspension culture.

Recent research shows that spheroids can be used as building blocks to bioprint tissues or organs (Mironov et al., 2003; Mironov et al., 2009; Mironov et al., 2011;

Laschke and Menger, 2016). Uniform spheroids are important as building blocks. Current methods to prepare these building blocks include hanging drops, microfluidics, micro-molds, spinner suspension culture, and rotating wall vessels (Mironov et al., 2009; Mironov et al., 2011; Olsen and Alexis, 2014; Laschke and Menger, 2016). With the hanging drop method, small volumes of cell suspensions are placed on a lid that is subsequently inverted to form hanging drops. Cells in each hanging drop aggregate to form one spheroid. With the microfluidic and micro-mold methods, cells are placed in micro-wells to form one spheroid per well. With the spinner culture and rotating wall vessel methods, large numbers of cells are cultured in suspension in the spinner flasks or rotating wall vessels to simultaneously generate many spheroids. The microfluidics, hanging drop, and micro-molds cannot produce spheroids at a large scale (Olsen and Alexis, 2014). 3D suspension is the scalable method to produce spheroids but suffers from spheroid agglomeration. We believe the molecular coating method described in this study can be used to address the problem. (Takahashi et al., 2007), (Shi et al., 2017)

Data availability statement

The original contributions presented in the study are included in the article/supplementary material further inquiries can be directed to the corresponding author.

Author contributions

Author YL: Conceived and designed the analysis. Draft the paper. Author QI: Collected the data. Performed the analysis. Author YP: Collected the data. Author LH: Performed the analysis and revised manuscript. Author YY and XW: Collected the data.

Funding

Research reported in this publication was supported by the National Heart, Lung, and Blood Institute of the National Institutes of Health under Award Number R33HL163711; and the National Cancer Institute under Award Number R33CA235326.

Conflict of interest

The authors declare that the research was conducted in the absence of any commercial or financial relationships that could be construed as a potential conflict of interest.

Publisher's note

All claims expressed in this article are solely those of the authors and do not necessarily represent those of their affiliated

organizations, or those of the publisher, the editors and the reviewers. Any product that may be evaluated in this article, or claim that may be made by its manufacturer, is not guaranteed or endorsed by the publisher.

References

- Alvarez-Pérez, J., Ballesteros, P., and Cerdán, S. (2005). Microscopic images of intraspheroidal pH by 1H magnetic resonance chemical shift imaging of pH sensitive indicators. *Magn. Reson. Mater. Phys. Biol. Med.* 18 (6), 293–301. doi:10.1007/s10334-005-0013-z
- Ambasudhan, R., Ryan, S. D., Dolatabadi, N., Chan, S. F., Zhang, X., Akhtar, M. W., et al. (2013). Isogenic human iPSC Parkinson's model shows nitrosative stress-induced dysfunction in MEF2-pgc1 α transcription. *Cell* 155 (6), 1351–1364. doi:10.1016/j.cell.2013.11.009
- Amour, K. A. D., Bang, A. G., Eliazar, S., Kelly, O. G., Agulnick, A. D., Smart, N. G., et al. (2006). Production of pancreatic hormone – expressing endocrine cells from human embryonic stem cells. *Nat. Biotechnol.* 24 (11), 1392–1401. doi:10.1038/nbt1259
- Badylak, S. F., Taylor, D., and Uygun, K. (2011). Whole-organ tissue engineering: Decellularization and recellularization of three-dimensional matrix scaffolds. *Annu. Rev. Biomed. Eng.* 13, 27–53. doi:10.1146/annurev-bioeng-071910-124743
- Barker, R. A., Parmar, M., Studer, L., and Takahashi, J. (2017). Human trials of stem cell-derived dopamine neurons for Parkinson's disease: Dawn of a new era. *Cell Stem Cell* 21 (5), 569–573. doi:10.1016/j.stem.2017.09.014
- Baum, E., Littman, N., Ruffin, M., Ward, S., and Aschheim, K. (2013). Key tools and technology hurdles in advancing stem-cell therapies. AvailableAt: <https://www.cirm.ca.gov/sites/default/files/files/>.
- Brennand, K. J., Simone, A., Jou, J., Gelboin-Burkhart, C., Tran, N., Sangar, S., et al. (2011). Modelling schizophrenia using human induced pluripotent stem cells. *Nature* 473 (7346), 221–225. doi:10.1038/nature09915
- Bright, J., Hussain, S., Dang, V., Wright, S., Cooper, B., Byun, T., et al. (2015). Human secreted tau increases amyloid-beta production. *Neurobiol. Aging* 36 (2), 693–709. doi:10.1016/j.neurobiolaging.2014.09.007
- Burridge, P. W., Li, Y. F., Matsa, E., Wu, H., Ong, S. G., Sharma, A., et al. (2016). Human induced pluripotent stem cell-derived cardiomyocytes recapitulate the predilection of breast cancer patients to doxorubicin-induced cardiotoxicity. *Nat. Med.* 22 (5), 547–556. doi:10.1038/nm.4087
- Chayosumrit, M., Tuch, B., and Sidhu, K. (2010). Alginate microcapsule for propagation and directed differentiation of hESCs to definitive endoderm. *Biomaterials* 31 (3), 505–514. doi:10.1016/j.biomaterials.2009.09.071
- Chen, K. G., Mallon, B. S., Johnson, K. R., Hamilton, R. S., McKay, R. D. G., and Robey, P. G. (2014). Developmental insights from early mammalian embryos and core signaling pathways that influence human pluripotent cell growth and differentiation. *Stem Cell Res.* 12 (3), 610–621. doi:10.1016/j.scr.2014.02.002
- Chen, K. G., Mallon, B. S., McKay, R. D. G., and Robey, P. G. (2014). Human pluripotent stem cell culture: Considerations for maintenance, expansion, and therapeutics. *Cell Stem Cell*, 14 (1), 13–26. doi:10.1016/j.stem.2013.12.005
- Chong, J. J. H., Yang, X., Don, C. W., Minami, E., Liu, Y.-W., Weyers, J. J., et al. (2014). Human embryonic-stem-cell-derived cardiomyocytes regenerate non-human primate hearts. *Nature* 510 (7504), 273–7. doi:10.1038/nature13233
- Deinsberger, J., Reisinger, D., and Weber, B. (2020). Global trends in clinical trials involving pluripotent stem cells: A systematic multi-database analysis. *npj Regen. Med.* 5 (1), 15–13. doi:10.1038/s41536-020-00100-4
- Denning, C., Borgdorff, V., Crutchley, J., Firth, K. S. A., George, V., Kalra, S., et al. (2016). Cardiomyocytes from human pluripotent stem cells: From laboratory curiosity to industrial biomedical platform. *Biochimica Biophysica Acta - Mol. Cell Res.* 1863 (7), 1728–1748. doi:10.1016/j.bbamcr.2015.10.014
- Desbordes, S. C., and Studer, L. (2012). Adapting human pluripotent stem cells to high-throughput and high-content screening. *Nat. Protoc.* 8 (1), 111–130. doi:10.1038/nprot.2012.139
- Devine, M. J., Rytan, M., Vodicka, P., Thomson, A. J., Burdon, T., Houlden, H., et al. (2011). Parkinson's disease induced pluripotent stem cells with triplication of the α -synuclein locus. *Nat. Commun.* 2 (1), 440–40. doi:10.1038/ncomms1453
- Ekerdt, B. L., Fuentes, C. M., Lei, Y., Adil, M. M., Ramasubramanian, A., Segalman, R. A., et al. (2018). Thermoreversible hyaluronic acid-PNIPAAm hydrogel systems for 3D stem cell culture. *Adv. Healthc. Mat.* 7, e1800225. doi:10.1002/adhm.201800225
- Foty, R. a., and Steinberg, M. S. (2005). The differential adhesion hypothesis: A direct evaluation. *Dev Biol* 278 (1), 255–63. doi:10.1016/j.ydbio.2004.11.012
- Fridley, K. M., Kinney, M. A., and McDevitt, T. C. (2012). Hydrodynamic modulation of pluripotent stem cells. *Stem Cell Res. Ther.* 3 (6), 45. doi:10.1186/scrt136
- Gerecht, S., Burdick, J. a., Ferreira, L. S., Townsend, S. a., Langer, R., and Vunjak-Novakovic, G. (2007). Hyaluronic acid hydrogel for controlled self-renewal and differentiation of human embryonic stem cells. *Proc. Natl. Acad. Sci. U. S. A.* 104 (27), 11298–11303. doi:10.1073/pnas.0703723104
- Hajdu, Z., Mironov, V., Mehesz, A. N., Norris, R. A., Markwald, R. R., and Visconti, R. P. (2010). Tissue spheroid fusion-based *in vitro* screening assays for analysis of tissue maturation. *J. Tissue Eng. Regen. Med.* 4, 659–664. doi:10.1002/term.291
- Hartman, M. E., Dai, D., and La, M. A. (2016). Human pluripotent stem cells: Prospects and challenges as a source of cardiomyocytes for *in vitro* modeling and cell-based cardiac repair. *Adv. Drug Deliv. Rev.* 96, 3–17. doi:10.1016/j.addr.2015.05.004
- Höing, S., Rudhard, Y., Reinhardt, P., Glatza, M., Stehling, M., Wu, G., et al. (2012). Discovery of inhibitors of microglial neurotoxicity acting through multiple mechanisms using a stem-cell-based phenotypic assay. *Cell Stem Cell* 11 (5), 620–632. doi:10.1016/j.stem.2012.07.005
- Inui, O., Teramura, Y., and Iwata, H. (2010). Retention dynamics of amphiphilic polymers PEG-lipids and PVA-Alkyl on the cell surface. *ACS Appl. Mat. Interfaces* 2 (5), 1514–1520. doi:10.1021/am100134v
- Israel, M. A., Yuan, S. H., Bardy, C., Reyna, S. M., Mu, Y., Herrera, C., et al. (2012). Probing sporadic and familial Alzheimer's disease using induced pluripotent stem cells. *Nature* 482 (7384), 216–220. doi:10.1038/nature10821
- Ivascu, A., and Kubbies, M. (2007). Diversity of cell-mediated adhesions in breast cancer spheroids. *Int. J. Oncol.* 11, 1403–1413. doi:10.3892/ijo.31.6.1403
- Ivascu, a., and Kubbies, M. (2006). Rapid generation of single-tumor spheroids for high-throughput cell function and toxicity analysis. *SLAS Discov.* 11 (8), 922–932. doi:10.1177/1087057106292763
- Jara-avaca, M., Kempf, H., Olmer, R., Kropp, C., Ru, M., Robles-diaz, D., et al. (2014). Controlling expansion and cardiomyogenic differentiation of human pluripotent stem cells in scalable suspension culture. *Stem Cell Rep.* 3, 1132–1146. doi:10.1016/j.stemcr.2014.09.017
- Jenkins, M. J., and Farid, S. S. (2015). Human pluripotent stem cell-derived products: Advances towards robust, scalable and cost-effective manufacturing strategies. *Biotechnol. J.* 10, 83–95. doi:10.1002/biot.201400348
- Kempf, H., Andree, B., and Zweigerdt, R. (2016). Large-scale production of human pluripotent stem cell derived cardiomyocytes. *Adv. Drug Deliv. Rev.* 96, 18–30. doi:10.1016/j.addr.2015.11.016
- Kikuchi, T., Morizane, A., Doi, D., Magotani, H., Onoe, H., Hayashi, T., et al. (2017). Human iPSC cell-derived dopaminergic neurons function in a primate Parkinson's disease model. *Nature* 548 (7669), 592–596. doi:10.1038/nature23664
- Kimbrel, E. A., and Lanza, R. (2015). Current status of pluripotent stem cells: Moving the first therapies to the clinic. *Nat. Rev. Drug Discov.* 14 (10), 681–692. doi:10.1038/nrd4738
- Kinney, M. A., Sargent, C. Y., and Mcdevitt, T. C. (2011). The multiparametric effects of hydrodynamic environments on stem cell culture. *Tissue Eng. Part B Rev.* 17, 249–262. doi:10.1089/ten.teb.2011.0040
- Kodo, K., Ong, S. G., Jahanbani, F., Termglinchan, V., Hirano, K., Inanloorahatloo, K., et al. (2016). iPSC-derived cardiomyocytes reveal abnormal TGF- β signalling in left ventricular non-compaction cardiomyopathy. *Nat. Cell Biol.* 18 (10), 1031–1042. doi:10.1038/ncb3411
- Kondo, T., Asai, M., Tsukita, K., Kutoku, Y., Ohsawa, Y., Sunada, Y., et al. (2013). Modeling Alzheimer's disease with iPSCs reveals stress phenotypes associated with intracellular A β and differential drug responsiveness. *Cell Stem Cell* 12 (4), 487–496. doi:10.1016/j.stem.2013.01.009

- Kropp, C., Massai, D., and Zweigerdt, R. (2017). Progress and challenges in large-scale expansion of human pluripotent stem cells. *Process Biochem.* 59, 244–254. doi:10.1016/j.procbio.2016.09.032
- Kumari, D., Swaroop, M., Southall, N., Huang, W., Zheng, W., and Usdin, K. (2015). High-throughput screening to identify compounds that increase fragile X mental retardation protein expression in neural stem cells differentiated from fragile X syndrome patient-derived induced pluripotent stem cells. *Stem Cells Transl. Med.* 4 (7), 800–808. doi:10.5966/sctm.2014-0278
- Laschke, M. W., and Menger, M. D. (2016). Life is 3D : Boosting spheroid function for tissue engineering. *Trends Biotechnol.* 35, 133–144. doi:10.1016/j.tibtech.2016.08.004
- Lei, Y., Jeong, D., Xiao, J., and Schaffer, D. V. (2014). Developing defined and scalable 3D culture systems for culturing human pluripotent stem cells at high densities. *Cell. Mol. Bioeng.* 7 (2), 172–183. doi:10.1007/s12195-014-0333-z
- Lei, Y., and Schaffer, D. V. (2013). A fully defined and scalable 3D culture system for human pluripotent stem cell expansion and differentiation. *Proc. Natl. Acad. Sci. U. S. A.* 110, E5039–E5048. doi:10.1073/pnas.1309408110
- Li, Q., Lin, H., Du, Q., Liu, K., Wang, O., Evans, C., et al. (2018). Scalable and physiologically relevant microenvironments for human pluripotent stem cell expansion and differentiation. *Biofabrication* 10, 25006. doi:10.1088/1758-5090/aa6b5
- Li, Q., Lin, H., Wang, O., Qiu, X., Kidambi, S., Deleyrolle, L. P., et al. (2016). Scalable production of glioblastoma tumor-initiating cells in 3 dimension thermoreversible hydrogels. *Sci. Rep.* 6, 31915. doi:10.1038/srep31915
- Lin, H., Du, Q., Li, Q., Wang, O., Wang, Z., Elowsky, C., et al. (2019). Manufacturing human pluripotent stem cell derived endothelial cells in scalable and cell-friendly microenvironments. *Biomater. Sci.* 7, 373–388. doi:10.1039/c8bm01095a
- Lin, H., Du, Q., Li, Q., Wang, O., Wang, Z., Liu, K., et al. (2018). Hydrogel-based bioprocess for scalable manufacturing of human pluripotent stem cell-derived neural stem cells. *ACS Appl. Mat. Interfaces* 10, 29238–29250. doi:10.1021/acsami.8b05780
- Lin, H., Du, Q., Li, Q., Wang, O., Wang, Z., Sahu, N., et al. (2018). A scalable and efficient bioprocess for manufacturing human pluripotent stem cell-derived endothelial cells. *Stem Cell Rep.* 11 (2), 454–469. doi:10.1016/j.stemcr.2018.07.001
- Lin, H., Li, Q., Du, Q., Wang, O., Wang, Z., Akert, L., et al. (2019). Integrated generation of induced pluripotent stem cells in a low-cost device. *Biomaterials*, 189, 23–36. doi:10.1016/j.biomaterials.2018.10.027
- Lin, H., Li, Q., and Lei, Y. (2017). An integrated miniature bioprocessing for personalized human induced pluripotent stem cell expansion and differentiation into neural stem cells. *Sci. Rep.* 7, 40191. doi:10.1038/srep40191
- Lin, H., Li, Q., and Lei, Y. (2017). Three-dimensional tissues using human pluripotent stem cell spheroids as biofabrication building blocks. *Biofabrication* 9, 25007. doi:10.1088/1758-5090/aa663b
- Lin, H., Qiu, X., Du, Q., Li, Q., Wang, O., Akert, L., et al. (2019). Engineered Microenvironment for Manufacturing Human Pluripotent Stem Cell-Derived Vascular Smooth Muscle Cells. *Stem Cell Reports*, 8, 84–97. doi:10.1016/j.stemcr.2018.11.009
- Lin, R. Z., and Chang, H. Y. (2008). Recent advances in three-dimensional multicellular spheroid culture for biomedical research. *Biotechnol. J.* 3 (9–10), 1285–1384. doi:10.1002/biot.1285
- Magdy, T., Schuldt, A. J. T., Wu, J. C., Bernstein, D., and Burridge, P. W. (2018). Human induced pluripotent stem cell (hiPSC)-derived cells to assess drug cardiotoxicity: Opportunities and problems. *Annu. Rev. Pharmacol. Toxicol.* 58, 83–103. doi:10.1146/annurev-pharmtox-010617-053110
- Mandai, M., Watanabe, A., Kurimoto, Y., Hirami, Y., Morinaga, C., Daimon, T., et al. (2017). Autologous induced stem-cell-derived retinal cells for macular degeneration. *N. Engl. J. Med. Overseas. Ed.* 376 (11), 1038–1046. doi:10.1056/NEJMoa1608368
- Matsa, E., Ahrens, J. H., and Wu, J. C. (2016). Human induced pluripotent stem cells as a platform for personalized and precision cardiovascular medicine. *Physiol. Rev.* 96 (3), 1093–1126. doi:10.1152/physrev.00036.2015
- Matsa, E., Burridge, P. W., Yu, K. H., Ahrens, J. H., Termglinchan, V., Wu, H., et al. (2016). Transcriptome profiling of patient-specific human iPSC-cardiomyocytes predicts individual drug safety and efficacy responses *in vitro*. *Cell Stem Cell* 19 (3), 311–325. doi:10.1016/j.stem.2016.07.006
- McNeish, J., Gardner, J. P., Wainger, B. J., Woolf, C. J., and Eggan, K. (2015). From dish to bedside: Lessons learned while translating findings from a stem cell model of disease to a clinical trial. *Cell Stem Cell* 17 (1), 8–10. doi:10.1016/j.stem.2015.06.013
- Mironov, V., Boland, T., Trusk, T., Forgacs, G., and Markwald, R. R. (2003). Organ printing: Computer-aided jet-based 3D tissue engineering. *Trends Biotechnol.* 21 (4), 157–161. doi:10.1016/s0167-7799(03)00033-7
- Mironov, V., Kasyanov, V., and Markwald, R. R. (2011). Organ printing: From bioprinter to organ biofabrication line. *Curr. Opin. Biotechnol.* 22 (5), 667–673. doi:10.1016/j.copbio.2011.02.006
- Mironov, V., Visconti, R. P., Kasyanov, V., Forgacs, G., Drake, C. J., and Markwald, R. R. (2009). Organ printing: Tissue spheroids as building blocks. *Biomaterials* 30 (12), 2164–2174. doi:10.1016/j.biomaterials.2008.12.084
- Mount, N. M., Ward, S. J., Kefalas, P., and Hyllner, J. (2015). Cell-based therapy technology classifications and translational challenges. *Phil. Trans. R. Soc. B* 370 (1680), 20150017. doi:10.1098/rstb.2015.0017
- Naryshkin, N. a., Weetall, M., Dakka, A., Narasimhan, J., Zhao, X., Feng, Z., et al. (2014). SMN2 splicing modifiers improve motor function and longevity in mice with spinal muscular atrophy. *Science* 345 (6197), 688–693. doi:10.1126/science.1250127
- National Cell Manufacturing Consortium (2016). Achieving large-scale, cost-effective, reproducible manufacturing of high-quality cells. Available from: http://cellmanufacturingusa.org/sites/default/files/NCMC_Roadmap_021816_high_res-2.pdf.
- National science and technology council (2016). Advanced Manufacturing: A Snapshot of Priority Technology Areas Across the Federal Government. Available from: https://www.whitehouse.gov/sites/whitehouse.gov/files/images/Blog/NSTC_SAM_technology_areas_snapshot.pdf.
- New Brunswick ScientificGouzheng, W., Zhang, W., Rich, M., and Gossain, V. (2009). Growing CHO cells in a CelliGen® BLU benchtop , stirred-tank bioreactor using single-use vessels. *Biotechnol. Prog.* 1, 4. doi:10.1038/nmeth.f.277
- Olsen, T. R., and Alexis, F. (2014). Bioprocess. *Tissues using Cell. Spheroids* 4 (2), 2–5. doi:10.4172/2155-9821.1000e112
- Park, I-H., Zhao, R., West, J. a., Yabuuchi, A., Huo, H., Ince, T. a., et al. (2008). Reprogramming of human somatic cells to pluripotency with defined factors. *Nature* 451, 141–146. doi:10.1038/nature06534
- Pérez-Pomares, J. M., and Foty, R. A. (2006). Tissue fusion and cell sorting in embryonic development and disease: Biomedical implications. *Bioessays*, 28(8): 809–21. doi:10.1002/bies.20442
- Polak, J. M., and Mantalaris, S. (2008). Stem cells bioprocessing : An important milestone to move regenerative medicine research into the clinical arena. *Pediatr. Res.* 63, 461–466. doi:10.1203/pdr.0b013e31816a8c1c
- Reinhardt, P., Schmid, B., Burbulla, L. F., Schöndorf, D. C., Wagner, L., Glatza, M., et al. (2013). Genetic correction of a Lrrk2 mutation in human iPSCs links parkinsonian neurodegeneration to ERK-dependent changes in gene expression. *Cell Stem Cell* 12 (3), 354–367. doi:10.1016/j.stem.2013.01.008
- Sayed, N., Liu, C., and Wu, J. C. (2016). Translation of human-induced Pluripotent Stem cells. *J. Am. Coll. Cardiol.* 67 (18), 2161–2176. doi:10.1016/j.jacc.2016.01.083
- Serra, M., Brito, C., Correia, C., and Alves, P. M. (2012). Process engineering of human pluripotent stem cells for clinical application. *Trends Biotechnol.* 30 (6), 350–359. doi:10.1016/j.tibtech.2012.03.003
- Serra, M., Correia, C., Malpique, R., Brito, C., Jensen, J., Bjoquist, P., et al. (2011). Microencapsulation technology: A powerful tool for integrating expansion and cryopreservation of human embryonic stem cells. *PLoS One* 6 (8), e23212. doi:10.1371/journal.pone.0023212
- Sharma, A., Burridge, P. W., Mckeithan, W. L., Serrano, R., Shukla, P., Sayed, N., et al. (2017). High-throughput screening of tyrosine kinase inhibitor cardiotoxicity with human induced pluripotent stem cells. *Sci. Transl. Med.* 9 (377), eaaf2584. doi:10.1126/scitranslmed.aaf2584
- Shi, Y., Inoue, H., Wu, J. C., and Yamanaka, S. (2017). Induced pluripotent stem cell technology: A decade of progress. *Nat. Rev. Drug Discov.* 16 (2), 115–130. doi:10.1038/nrd.2016.245
- Silva, M., Dameron, L., Hurlley, H., Bure, K., Barker, R., Carr, A. J., et al. (2015). Generating iPSCs: Translating cell reprogramming science into scalable and robust biomufacturing strategies. *Cell Stem Cell* 16 (1), 13–17. doi:10.1016/j.stem.2014.12.013
- Soldner, F., Stelzer, Y., Shivalila, C. S., Abraham, B. J., Latourelle, J. C., Barrasa, M. I., et al. (2016). Parkinson-associated risk variant in distal enhancer of α -synuclein modulates target gene expression. *Nature* 533 (7601), 95–99. doi:10.1038/nature17939
- Stenberg, J., Elvsson, M., Strehl, R., Kilmare, E., Hyllner, J., and Lindahl, A. (2011). Sustained embryoid body formation and culture in a non-laborious three dimensional culture system for human embryonic stem cells. *Cytotechnology* 63 (3), 227–237. doi:10.1007/s10616-011-9344-y

- Tabar, V., and Studer, L. (2014). Pluripotent stem cells in regenerative medicine: Challenges and recent progress. *Nat. Rev. Genet.* 15 (2), 82–92. doi:10.1038/nrg3563
- Takahashi, K., Tanabe, K., Ohnuki, M., Narita, M., Ichisaka, T., Tomoda, K., et al. (2007). Induction of pluripotent stem cells from adult human fibroblasts by defined factors. *Cell* 131 (5), 861–872. doi:10.1016/j.cell.2007.11.019
- Takemoto, N., Teramura, Y., and Iwata, H. (2011). Islet surface modification with urokinase through DNA hybridization. *Bioconjug. Chem.* 22 (4), 673–678. doi:10.1021/bc100453r
- Tatsumi, K., Ohashi, K., Teramura, Y., Utoh, R., Kanegae, K., Watanabe, N., et al. (2012). The non-invasive cell surface modification of hepatocytes with PEG-lipid derivatives. *Biomaterials* 33 (3), 821–828. doi:10.1016/j.biomaterials.2011.10.016
- Teramura, Y., and Iwata, H. (2010). Bioartificial pancreas. *Adv. Drug Deliv. Rev.* 62 (7–8), 827–840. doi:10.1016/j.addr.2010.01.005
- Teramura, Y., and Iwata, H. (2010). Cell surface modification with polymers for biomedical studies. *Soft Matter*. 6 (6), 1081. doi:10.1039/b913621e
- Thomson, J. A., Itskovitz-Eldor, J., Shapiro, S. S., Waknitz, M. A., Swiergiel, J. J., Marshall, V. S., et al. (1998). Embryonic stem cell lines derived from human blastocysts. *Science* 282, 1145–1147. doi:10.1126/science.282.5391.1145
- Trainor, N., Pietak, A., and Smith, T. (2014). Rethinking clinical delivery of adult stem cell therapies. *Nat. Biotechnol.* 32 (8), 729–735. doi:10.1038/nbt.2970
- Trounson, A., and McDonald, C. (2015). Stem cell therapies in clinical trials: Progress and challenges. *Cell Stem Cell* 17 (1), 11–22. doi:10.1016/j.stem.2015.06.007
- Wang, O., and Lei, Y. (2019). Creating a cell-friendly microenvironment to enhance cell culture efficiency. *Cell Gene Ther. Insights* 5 (3), 341–350. doi:10.18609/cgti.2019.038
- Wang, Z., Zuo, F., Liu, Q., Wu, X., Du, Q., Lei, Y., et al. (2021). Comparative study of human pluripotent stem cell-derived endothelial cells in hydrogel-based culture systems. *ACS Omega* 6 (10), 6942–6952. doi:10.1021/acsomega.0c06187
- Woodruff, G., Young, J. E., Martinez, F. J., Buen, F., Gore, A., Kinaga, J., et al. (2013). The Presenilin-1 δ E9 mutation results in reduced γ -secretase activity, but not total loss of PS1 function, in isogenic human stem cells. *Cell Rep.* 5 (4), 974–985. doi:10.1016/j.celrep.2013.10.018
- Yamanaka, S. (2020). Pluripotent stem cell-based cell therapy—promise and challenges. *Cell Stem Cell* 27 (4), 523–531. doi:10.1016/j.stem.2020.09.014
- Young, J. E., Boulanger-Weill, J., Williams, D. A., Woodruff, G., Buen, F., Revilla, A. C., et al. (2015). Elucidating molecular phenotypes caused by the SORL1 Alzheimer's disease genetic risk factor using human induced pluripotent stem cells. *Cell Stem Cell* 16 (4), 373–385. doi:10.1016/j.stem.2015.02.004